Aggregation Behavior of Amphiphilic Dendritic Block Copolymer with Butanediyl-α,ω-bis(tetradecyldimethylammonium bromide) in Aqueous Solution†

Changchao Hu,‡ Hui Yang,‡ Rongqiang Li,‡,§ Xu Wu,‡ and Jinben Wang*,‡

Beijing National Laboratory for Molecular Sciences, Key Laboratory of Colloid, Interface and Chemical Thermodynamics, Institute of Chemistry, Chinese Academy of Sciences, Beijing 100190, People's Republic of China, and School of Chemical and Environmental Engineering, China University of Mining and Technology (Beijing), Beijing 100083, People's Republic of China

Aggregation behavior of an amphiphilic dendritic block copolymer, a generation 1.0 poly(amidoamine) (G1.0 PAMAM) dendrimer based poly(propylene oxide) (PPO)-block-poly(ethylene oxide) (PEO) copolymer that was abbreviated as PPP, with a cationic gemini surfactant butanediyl-α,ω-bis(tetradecyldimethylammonium bromide) (14-4-14) in aqueous solution was investigated by the measurements of steady-state fluorescence (FL), cloud point (CP), transmission electron microscope (TEM), and dynamic light scattering (DLS). Through FL method, the critical aggregation concentration (CAC) of PPP in the absence and presence of 14-4-14 was determined. As the concentration of 14-4-14 increases, CAC values increase, suggesting the participation of copolymer−surfactant complexes in aggregate formation. The CP temperature of PPP increases as the content of 14-4-14 increases in the mixed system, which indicates that 14-4-14 increases the solubility of PPP. From TEM and DLS, the morphology and size distribution of the aggregates were obtained. The spherical aggregates are found to be larger in size and narrower in distribution with the addition of 14-4-14, which confirms further the formation of mixed aggregates. All of the above are explained on the basis of strong interactions between PPP and 14-4-14. Through hydrophobic interactions, 14-4-14 molecules can associate with PPP molecules to form copolymer−surfactant complexes that can aggregate further.

Introduction

Dendrimers, possessing distinctive properties such as globular architectures, narrow polydispersity (often uniquely monodisperse), compatibility, and tunability of surface functional groups, are a novel series of highly branched macromolecules, consisting of a central core and radial attached branching units which lead to a spherical periphery and controlled terminal groups.[1,2] Since the successful synthesis in 1985, dendrimers have attracted considerable attention because of their various chemical compositions, available synthetic methodologies, unique structures, and versatility, which render them a reliable alternative to traditional linear polymers in a wide range of applications.[3,4] Up to now, they have been used as hosts in host−guest systems, drug capsules, gene delivery vehicles, cancer targeting platforms, nanomaterial synthesis templates, catalyst carriers, and so forth.[2,5–11]

Among the variety of dendrimers, the poly(aminoamide) (PAMAM) family is the most thoroughly investigated group. With a star-like shape, they have primary amine functional groups at each branch end point and tertiary amine groups at each branch dividing point, with the arms functionalized via covalent modifications further.[12–14] In recent years, interest is focused on the interactions between PAMAM dendrimers (or the derivatives) and surfactants due to the widespread applications of these mixed systems.[15,16] The morphology, nature, and interaction mechanism of the PAMAM/derivative surfactant aggregates have been reported by a few scientists.[17–20] For the mixed system of PAMAM/derivative and oppositely charged surfactant, through electrostatic interactions, a template-assisted supramolecular assembly consisting of a dendrimer/derivative at the core and amphiphilic surfactants on the surface is formed.[16] Surfactants can also penetrate the surface charge barriers of PAMAM dendrimers/derivatives and localize in their interior cavities by hydrophobic interactions or hydrogen-bonding interactions.[21] For systematic investigation and practical application,[22,23] it is worthwhile to study the aggregation behavior of PAMAM dendrimers branched with amphiphilic block copolymers with surfactants. To our knowledge, however, there is no report available. We have synthesized a series of PAMAM dendrimer based block copolymers and studied their aggregation properties in aqueous solutions in our earlier work.[24,25] To further our research, in the present work, we have characterized the aggregation behavior of an amphiphilic dendritic block copolymer (abbreviated as PPP) with a gemini surfactant (14-4-14) for the first time, with the methods of cloud point (CP), steady-state fluorescence (FL), dynamic light scattering (DLS), and transmission electron microscope (TEM). Interesting results from this study are expected to help us further understand the complex nature of copolymer−surfactant interactions from a fundamental point of view, which may be useful for potential applications.

Experimental Section

Materials. Pyrene was purchased from Aldrich and recrystallized from ethanol before use. *N*,*N*-Dimethyltetradecylamine was purchased from Tokyo Chemical Industry Co., Ltd. Ethylenediamine (EDA), methyl acrylate (MA), propylene oxide (PO), ethylene oxide (EO), α,ω-dibromobutane, and other chemicals

† Part of the "Sir John S. Rowlinson Festschrift".

* To whom correspondence should be addressed. Tel.: +86-10-62523395; fax: +86-10-62523395. E-mail: jbwang@iccas.ac.cn.
‡ Chinese Academy of Sciences.
§ China University of Mining and Technology (Beijing).

10.1021/je1003725
Published on Web 07/21/2010

Table 1. Polydispersity (M_w/M_n), Molecular Weight (M_w), Numbers of Propylene Oxide Unit (x), and Ethylene Oxide Unit (y) per Chain of PPP

M_w/M_n	M_w/g·L^{-1}	x	y
1.22	26700[a]	30	10

[a] Apparent molecular weight which is obtained from GPC.

were obtained from Beijing Chemical Co. and were of analytical grade. All of the solutions were prepared with triply distilled water.

Synthesis and Characterization. G1.0 PAMAM dendrimer was synthesized through a divergent approach.[26] Briefly, EDA was dissolved in methanol and added dropwise to purified MA (excess) under N_2 atmosphere. The reaction was carried out for 24 h at 303.15 K with an agitator. The methanol and unreacted MA were removed under vacuum, and G0.5 PAMAM dendrimer was obtained. Then, the G0.5 PAMAM dendrimer was dissolved in methanol and added dropwise to EDA (excess). After keeping for 24 h at 303.15 K with an agitator, the methanol and unreacted EDA were removed under vacuum, and G1.0 PAMAM dendrimer was obtained. PPP was synthesized by anionic polymerization.[22] In brief, PO was added into a reacting kettle containing G1.0 PAMAM dendrimer as initiator and potassium hydroxide as catalyst at 408.15 K and 0.4 MPa under N_2 atmosphere. Keeping the reaction for (3 to 5) h, EO was added, and the reaction was kept for another (3 to 5) h at 403.15 K and 0.4 MPa. After cooling down to 333.15 K, phosphoric acid was added to neutralize the added catalyst, and the product was obtained. Characterization of PPP was carried out as described in our earlier work.[24] The molecular weight distribution of PPP was determined by gel permeation chromatography (GPC) using a set equipped with a Waters 515 pump, a Waters 2414 refractive index detector, and a combination of three Styragel columns (HT2, HT3, and HT4). Tetrahydrofuran was used as eluent at a flow rate of 1.0 mL·min^{-1} at 308.15 K. Polystyrene standards were used for calibration. The key characteristic parameters of PPP were listed in Table 1. 14-4-14 was synthesized according to the literature method.[27] Briefly, α,ω-dibromobutane was refluxed with *N*,*N*-dimethyltetradecylamine in dry acetone for 24 h. The product was obtained through filtration and recrystallized thrice from acetone. The purity was checked by ^{1}H NMR using a Bruker AV-400 NMR spectrometer, which gave corrected chemical shifts and expected proton contents according to the ratios of integration areas. No impurity peak was found. From the ratios of integration areas, the purity of 14-4-14 was estimated to be no less than 0.98 (mole fraction). Structures of PPP and 14-4-14 were shown in Figures 1 and 2, respectively.

Cloud Point (CP) Measurement. The CP measurement was carried out on a Brinkmann PC920 colorimeter equipped with a Shimadau 1601 PC UV−vis spectrometer. The turbidity of 1 g·L^{-1} PPP solution was monitored by UV transmittance at 450 nm. The temperature of the PPP solution was controlled by a thermostatted water-circulating bath and raised gradually under constant stirring. The data were reported as turbidity = 100 − T, where T is transmittance (percent). The turbidity reading was checked at intervals of 0.2 K after it reached a steady value. CP temperature was obtained from the break of 100 − T versus temperature curve.

Steady-State Fluorescence (FL) Measurement. Pyrene was employed as a fluorescence probe at the concentration of 1 μM. It was excited at 335 nm, and the emission spectrum was scanned from (350 to 550) nm. I_1/I_3 is the ratio of fluorescence intensities of pyrene emission spectrum at 373 nm (the first peak) and 384 nm (the third peak), which was used to evaluate the variations of micropolarity of aggregates. Tests were carried out on a Hitachi F-4500 fluorescence spectrophotometer at 298.15 ± 0.5 K.

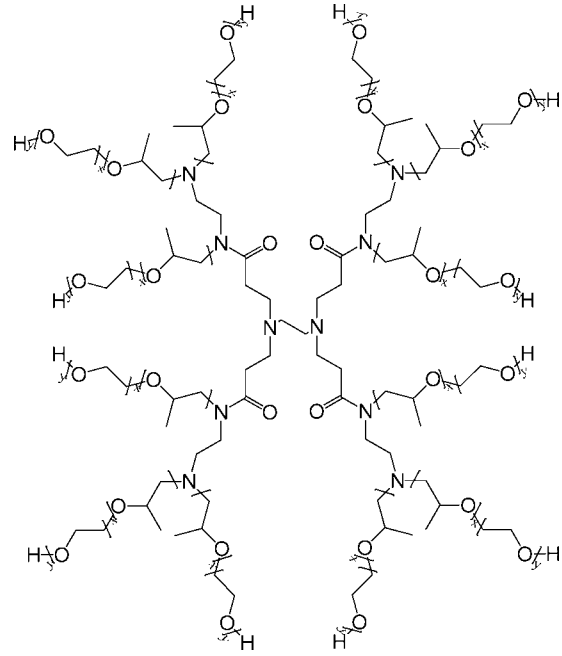

Figure 1. Scheme of PPP.

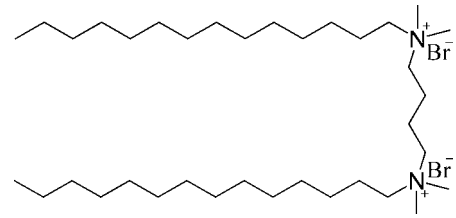

Figure 2. Scheme of 14-4-14.

Dynamic Light Scattering (DLS). DLS measurement was introduced, using a laser light scattering (LLS) spectrometer (ALV/SP-125) with a multi-τ digital time correlator (ALV-5000). Light (λ = 632.8 nm) from a cylindrical UNIPHASE He−Ne laser (22 mW) was used as the incident beam. The scattering angle was selected to 90°, and the correlation function was analyzed with the commercial CONTIN software provided by ALV.[28] Aqueous solutions of PPP (1 g·L^{-1}) with different concentrations of 14-4-14 were filtrated through 0.45 μm Millipores to leach dust before measurement.

Transmission Electron Microscope (TEM). Samples were prepared from 1 g·L^{-1} of PPP solution using a negative-staining method, and 5 g·L^{-1} of uranyl acetate aqueous solution was used as a staining agent. A drop of the solution was placed on a carbon Formvar-coated copper grid (300 mesh), and the excess liquid was sucked away by a filter paper. Then, the sample was negatively stained with the uranyl acetate aqueous solution. After drying, the samples were imaged under a JEM-200CX electron microscope at a working voltage of 100 kV.

Results and Discussion

The intensity ratio I_1/I_3 is used to investigate the polarity of the microenvironment of aggregates and determine the critical aggregation concentration (CAC).[29–31] Figure 3

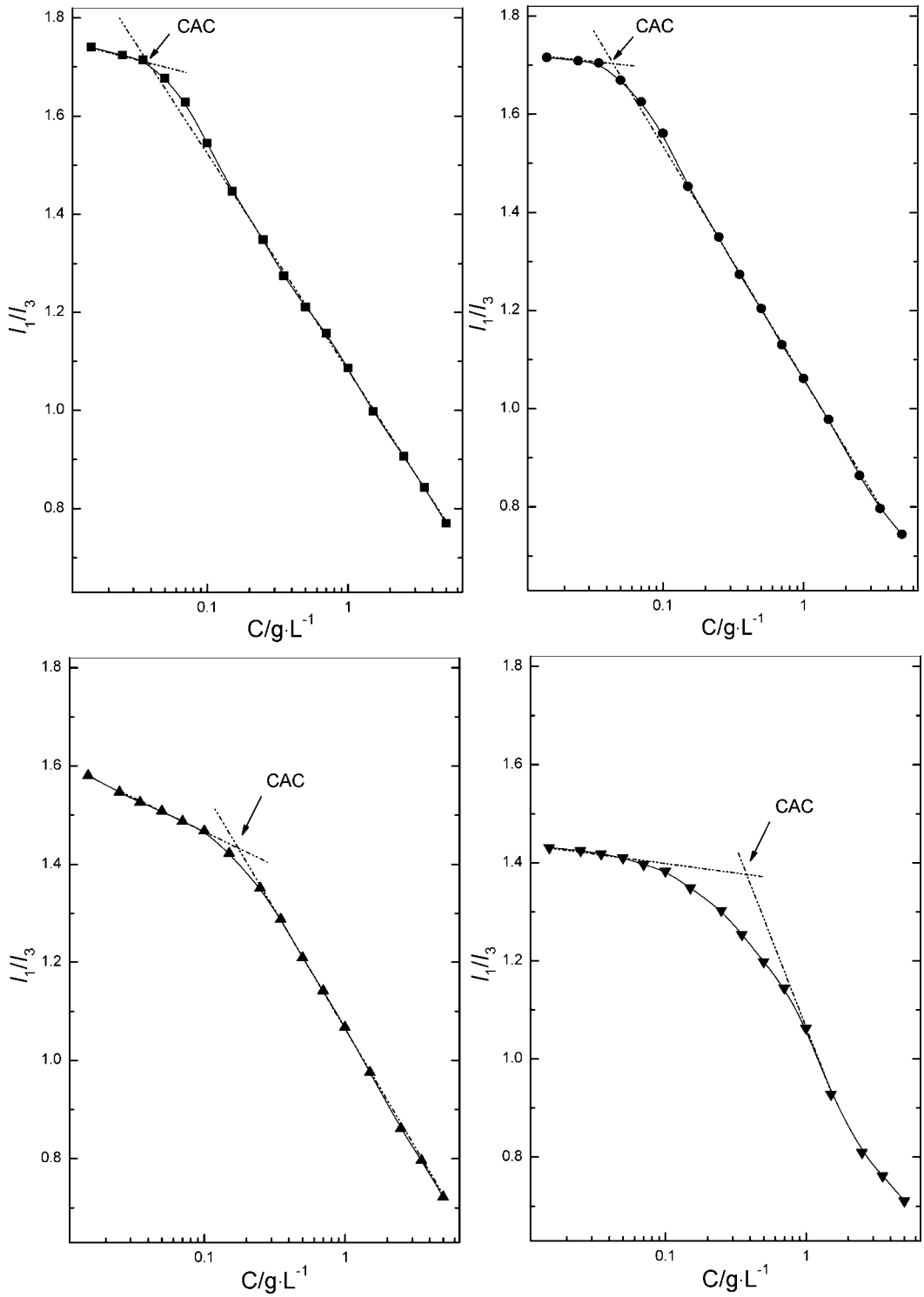

Figure 3. Variations of I_1/I_3 with the concentration (C) of PPP at different concentrations of 14-4-14: ■, 0 mM; ●, 0.0375 mM; ▲, 0.15 mM; ▼, 0.6 mM.

exhibits the variation of I_1/I_3 value as a function of PPP concentration in the absence and presence of 14-4-14. With the concentration of PPP increasing, I_1/I_3 of pyrene decreases slowly at the concentration below CAC and rapidly at higher concentration. The sharp break in the curve represents the transfer of pyrene from higher polar to lower and more hydrophobic environment, which corresponds to the formation of aggregates.[29,30] Thus, CAC can be determined through the break point, and the results are listed in Table 2. As the concentration of 14-4-14 increases from (0 to 0.6) mM (four times CMC of 14-4-14[32]), CAC values increase from (0.038

Table 2. Critical Aggregation Concentration (CAC), Hydration Radius (R_h), and Cloud Point (CP) for PPP Solution with Different Concentrations of 14-4-14

$C_{14\text{-}4\text{-}14}$ / mM	CAC / g·L^{-1}	R_h / nm	CP / K
0.0	0.038	2.5	297.25
0.0375	0.044	1, 44	309.45
0.15	0.17	70	> 343.15[a]
0.60	0.38	90	> 343.15[a]

[a] It was not possible to measure the CP of PPP solution at 14-4-14 concentrations of (0.15 and 0.6) mM.

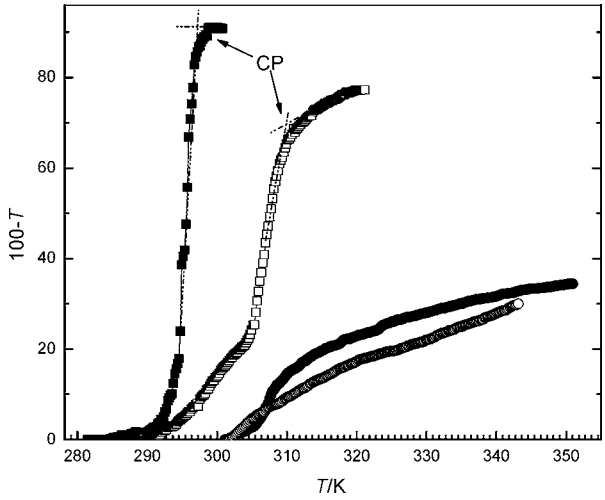

Figure 4. Turbidity ($100 - T$) versus temperature (T) curve of 1 g·L^{-1} PPP solution with different concentrations of 14-4-14: ■, 0 mM; □, 0.0375 mM; ●, 0.15 mM; ○, 0.6 mM.

to 0.38) g·L^{-1}. PPP molecules and 14-4-14 molecules may form copolymer−surfactant complexes with one PPP molecule associated with several 14-4-14 molecules through hydrophobic interactions, which corresponds to the slowly decreasing portion of the curve in Figure 3. The complexes can further form larger aggregates. With the concentration of 14-4-14 increasing, the loaded charges per complex increase, so the electrostatic repulsions between polar heads of the complexes increase, which leads to the higher aggregation concentration.

Figure 4 shows the variation of $100 - T$ versus temperature of PPP aqueous solution in the absence and presence of different concentrations of 14-4-14. CP temperature is determined from the break in the curve, and the values are listed in Table 2. Generally, as the temperature increasing, the hydrogen bonds between hydrophilic ethylene oxide units in the hydrophilic head groups of nonionic copolymer and water molecules are gradually destroyed, resulting in the decreasing of the solubility of nonionic copolymer. To a certain temperature, phase separation occurs, and the solution turns cloudy.[33,34] From Figure 4 and Table 2, it can be seen that the CP temperature of PPP increases as the concentration of 14-4-14 increases, indicating the solubility of PPP increases. This is most likely caused by increasing number of PPP molecules involved in the aggregation, which is consistent with the results from FL measurement. With the addition of 14-4-14 to PPP solution, more 14-4-14 molecules may penetrate into the interior of PPP molecules and associate cooperatively with the latter by replacing water molecules in the hydrophobic domains. The hydrophilic heads of 14-4-14 localize near PEO blocks, and the long hydrophobic tails of 14-4-14 localize near PPO blocks or in the relative nonpolar pockets of PPP core, which enhanced the hydrophilicity of PPP, and more PPP molecules participated in the formation of aggregates. The association is similar to that of PEO-PPO-PEO copolymers and gemini surfactants,[35,36] but different from that of charged block copolymers and oppositely charged gemini surfactants. For the latter, the association is induced by the electrostatic attraction.[37,38]

Representative TEM images of aggregates of PPP aqueous solution with and without different concentrations of 14-4-14 are shown in Figure 5. With the concentrations of 14-4-14 at (0.0375, 0.15, and 0.6) mM, spherical aggregates with

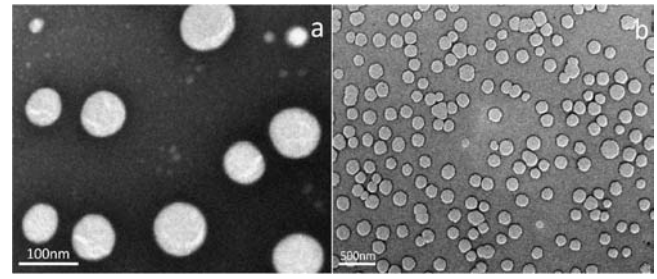

Figure 5. TEM images of the aggregates of 1 g·L^{-1} PPP solution with different concentrations of 14-4-14: (a) 0.0375 mM, (b) 0.6 mM.

about (100, 150, and 200) nm in diameter are observed, respectively, which suggests that larger aggregates should form with higher concentrations of 14-4-14. This is attributed to the structural transformation. With more 14-4-14 molecules penetrating into the interior of PPP, the enhanced electrostatic repulsions may lead to swollen conformation of PPP molecule.

To obtain the size and distribution of aggregates, PPP aqueous solution in the absence and presence of different concentrations of 14-4-14 is determined by DLS, as shown in Figure 6 and Table 2. It can be observed that the size of the aggregates of PPP in the absence of 14-4-14 shows a relatively broad distribution, with the average hydration radius (R_h) of about 2.5 nm. For PPP and 0.0375 mM 14-4-14, two R_h distributions are observed, with one centered at around 1 nm and the other at around 44 nm. The former may corresponds to aggregates of PPP, while the latter corresponds to mixed aggregates. When the concentration of 14-4-14 increases from (0.15 to 0.6) mM, R_h distributions become narrow, with R_h increasing from around (70 to 90) nm. The results agree well with that of TEM, indicating that 14-4-14 can interact with PPP and the content of the former has an important effect on morphology of the mixed aggregates. PPP molecules and 14-4-14 molecules may be able to form copolymer−surfactant complexes through hydrophobic interactions, and the complexes can form bigger aggregates. With the concentration of 14-4-14 increasing, more 14-4-14 molecules may participate in the formation of complexes, which leads to the higher values of CAC and CP temperature, as well as larger size and narrower distributions of the aggregates. It is worth mentioning that, at (0.15 and 0.6) mM, 14-4-14 can form free gemini micelles and vesicles itself. In Figure 6, the very weak peaks may attribute to the gemini micelles, while the peak of gemini vesicles (at around 35 nm, data not shown) may be overlapped by the peak of mixed aggregates.

Conclusions

The aggregation behavior of PPP with 14-4-14 in aqueous solution has been investigated at different concentrations of 14-4-14. As the concentration of 14-4-14 increases, FL results show an increase of CAC, and TEM and DLS results reveal that larger spherical aggregates with narrower distributions are formed. From CP measurement, it is found that the solubility of PPP is increased by 14-4-14. All of the present results indicate that there are strong interactions between PPP and 14-4-14, which can be explained that long hydrophobic tails of 14-4-14 may be able to associate with PPP through hydrophobic interactions, with the hydrophilic heads localizing near PEO blocks and the hydrophobic tails near PPO blocks or in the relative nonpolar cavities of PPP core to form copolymer−surfactant complexes that can form larger

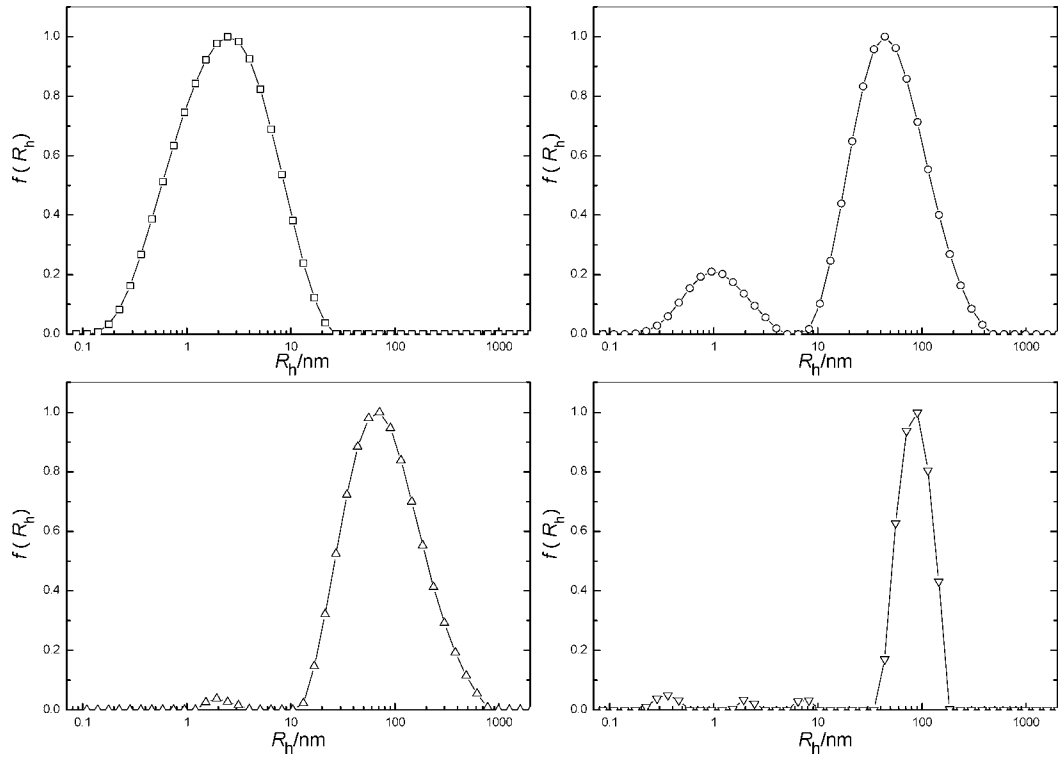

Figure 6. R_h distribution of 1 g·L^{-1} PPP solution with different concentrations of 14-4-14: □, 0 mM; ○, 0.0375 mM; △, 0.15 mM; ▽, 0.6 mM.

aggregates further. The interactions are strengthened by the addition of more 14-4-14.

Literature Cited

(1) Lopez, A. L.; Reins, R. Y.; McDermott, A. M.; Trautner, B. W.; Cai, C. Antibacterial Activity and Cytotoxicity of PEGylated Poly(amidoamine) Dendrimers. *Mol. BioSyst.* **2009**, *5*, 1148–1156.

(2) Tanis, I.; Karatasos, K. Molecular Dynamics Simulations of Polyamidoamine Dendrimers and Their Complexes with Linear Poly(ethylene oxide) at Different pH Conditions: Static Properties and Hydrogen Bonding. *Phys. Chem. Chem. Phys.* **2009**, *11*, 10017–10028.

(3) Wu, Q.; Cheng, Y.; Hu, J.; Zhao, L.; Xu, T. Insights into the Interactions between Dendrimers and Bioactive Surfactants: 3. Size-Dependent and Hydrophobic Property-Dependent Encapsulation of Bile Salts. *J. Phys. Chem. B* **2009**, *113*, 12934–12943.

(4) Zhang, W.; Simanek, E. E. Dendrimers Based on Melamine. Divergent and Orthogonal, Convergent Syntheses of a G3 Dendrimer. *Org. Lett.* **2000**, *2*, 843–845.

(5) Didehban, K.; Namazi, H.; Entezami, A. A. Dendrimer-based Hydrogen-bonded Liquid Crystalline Complexes: Synthesis and Characterization. *Eur. Polym. J.* **2009**, *45*, 1836–1844.

(6) Parimi, S.; Barnes, T. J.; Callen, D. F.; Prestidge, C. A. Mechanistic Insight into Cell Growth, Internalization and Cytotoxicity of PAMAM Dendrimers. *Biomacromolecules* **2010**, *11*, 11382–11389.

(7) Svenson, S. Dendrimers as Aersatile Platform in Drug Delivery Applications. *Eur. J. Pharm. Biopharm.* **2009**, *71*, 445–462.

(8) Al-Jamal, K. T.; Ramaswamy, C.; Florence, A. T. Supramolecular Structures from Dendrons and Dendrimers. *Adv. Drug Delivery Rev.* **2005**, *57*, 2238–2270.

(9) Örberg, M. L.; Schillén, K.; Nylander, T. Dynamic Light Scattering and Fluorescence Study of the Interaction between Double-Stranded DNA and Poly(amido amine) Dendrimers. *Biomacromolecules* **2007**, *8*, 1557–1563.

(10) Singh, P.; Gupta, U.; Asthana, A.; Jain, N. K. Folate and Folate-PEG-PAMAM Dendrimers: Synthesis, Characterization, and Targeted Anticancer Drug Delivery Potential in Tumor Bearing Mice. *Bioconjugate Chem.* **2008**, *19*, 2239–2252.

(11) Murugan, E.; Sherman, R. L.; Spivey, H. O.; Ford, W. T. Catalysis by Hydrophobically Modified Poly(propylenimine) Dendrimers Having Quaternary Ammonium and Tertiary Amine Functionality. *Langmuir* **2004**, *20*, 8307–8312.

(12) Ainalem, M. L.; Carnerup, A. M.; Janiak, J.; Alfredsson, V.; Nylander, T.; Schillén, K. Condensing DNA with Poly(amido amine) Dendrimers of Different Generations: Means of Controlling Aggregate Morphology. *Soft Matter* **2009**, *5*, 2310–2320.

(13) Yoshimura, T.; Abe, S.; Esum, K. Characterization of Quaternized Poly(amidoamine) Dendrimers of Generation 1 with Multiple Octyl Chains. *Colloid Surf., A* **2004**, *251*, 141–144.

(14) Esumi, K.; Hosoya, T.; Suzuki, A. Spontaneous Formation of Gold Nanoparticles in Aqueous Solution of Sugar-Persubstituted Poly-(amidoamine) Dendrimers. *Langmuir* **2000**, *16*, 2978–2980.

(15) Carbone, P.; Müller-Plathe, F. Molecular Dynamics Simulations of Polyaminoamide (PAMAM) Dendrimer Aggregates: Molecular Shape, Hydrogen Bonds and Local Dynamics. *Soft Matter* **2009**, *5*, 2638–2647.

(16) Cheng, Y.; Wu, Q.; Li, Y.; Hu, J.; Xu, T. New Insights into the Interactions between Dendrimers and Surfactants: 2. Design of New Drug Formulations Based on Dendrimer-Surfactant Aggregates. *J. Phys. Chem. B* **2009**, *113*, 8339–8346.

(17) Wang, C.; Wyn-Jones, E.; Sidhu, J.; Tam, K. C. Supramolecular Complex Induced by the Binding of Sodium Dodecyl Sulfate to PAMAM Dendrimers. *Langmuir* **2007**, *23*, 1635–1639.

(18) Bakshi, M. S.; Kaura, A.; Miller, J. D.; Paruchuri, V. K. Sodium Dodecyl Sulfate-poly(amidoamine) Interactions Studied by AFM Imaging, Conductivity, and Krafft Temperature Measurements. *J. Colloid Interface Sci.* **2004**, *278*, 472–477.

(19) Miyazaki, M.; Torigoe, K.; Esumi, K. Interactions of Sugar-Persubstituted Poly(Amidoamine) Dendrimers with Anionic Surfactants. *Langmuir* **2000**, *16*, 1522–1528.

(20) Bakshi, M. S.; Kaura, A.; Mahajan, R. K.; Yoshimura, T.; Esumi, K. Dodecyltrimethylammonium and Di(dodecyldimethylammonium) Bromides Interactions with Poly (amidoamine) Dendrimer. *Colloid Surf., A* **2004**, *246*, 39–48.

(21) Cheng, Y.; Li, Y.; Wu, Q.; Xu, T. New Insights into the Interactions between Dendrimers and Surfactants by Two Dimensional NOE NMR Spectroscopy. *J. Phys. Chem. B* **2008**, *112*, 12674–12680.

(22) Zhang, Z.; Xu, G.; Wang, F.; Dong, S.; Chen, Y. Demulsification by Amphiphilic Dendrimer Copolymers. *J. Colloid Interface Sci.* **2005**, *282*, 1–4.

(23) Xin, X.; Xu, G.; Zhang, Z.; Chen, Y.; Wang, F. Aggregation Behavior of Star-like PEO-PPO-PEO Block Copolymer in Aqueous Solution. *Eur. Polym. J.* **2007**, *43*, 3106–3111.

(24) Yang, H.; Han, Y.; Yang, S.; Zhang, W.; Tan, G.; Wang, Y.; Wang, J. Aggregation Behaviour of a Novel Series of Polyamidoamine-based Dendrimers. *Supramol. Chem.* **2009**, *21*, 754–758.

(25) Zhang, W.; Dong, G.; Yang, H.; Sun, J.; Zhou, J.; Wang, J. Synthesis, Surface and Aggregation Properties of a Series of Amphiphilic Dendritic Copolymers. *Colloid Surf., A* **2009**, *348*, 45–48.

(26) Tomalia, D. A.; Baker, H.; Dewald, J. A New Class of Polymers: Starburst-dendritic Macromolecules. *Polym. J.* **1985**, *17*, 117–132.
(27) Zana, R.; Benrraou, M.; Rueff, R. Alkanediyl-α,ω-bis(dimethylalkylammonium bromide) Surfactants. 1. Effect of the Spacer Chain Length on the Critical Micelle Concentration and Micelle Ionization Degree. *Langmuir* **1991**, *7*, 1072–1075.
(28) Provencher, S. W. CONTIN: a General Purpose Constrained Regularization Program for Inverting Noisy Linear Algebraic and Integral Equations. *Comput. Phys. Commun.* **1982**, *27*, 229–242.
(29) Hans, M.; Shimoni, K.; Danino, D.; Siegel, S. J.; Lowman, A. Synthesis and Characterization of mPEG-PLA Prodrug Micelles. *Biomacromolecules* **2005**, *6*, 2708–2717.
(30) Dutta, P.; Dey, J.; Ghosh, G.; Nayak, R. R. Self-association and Microenvironment of Random Amphiphilic Copolymers of Sodium *N*-acryloyl-l-valinate and *N*-dodecylacrylamide in Aqueous Solution. *Polymer* **2009**, *50*, 1516–1525.
(31) Kalyanasundaram, K.; Thomas, J. K. Environmental Effects on Vibronic Band Intensities in Pyrene Monomer Fluorescence and Their Application in Studies of Micellar Systems. *J. Am. Chem. Soc.* **1977**, *99*, 2039–2044.
(32) Azum, N.; Naqvi, A. Z.; Akram, M.; Kabir-ud-Din. Properties of Mixed Aqueous Micellar Solutions Formed by Cationic Alkanediyl-α,ω-bis(tetradecyldimethylammonium bromide) and Alkyltrimethylammonium Bromides: Fluorescence and Conductivity Studies. *J. Chem. Eng. Data* **2009**, *54*, 1518–1523.
(33) Zhao, G.; Chen, S. B. Clouding and Phase Behavior of Nonionic Surfactants in Hydrophobically Modified Hydroxyethyl Cellulose Solutions. *Langmuir* **2006**, *22*, 9129–9134.
(34) Kumar, S.; Aswal, V. K.; Naqvi, A. Z.; Goyal, P. S.; Kabir-ud-Din. Cloud Point Phenomenon in Ionic Micellar Solutions: a SANS Study. *Langmuir* **2001**, *17*, 2549–2551.
(35) Li, X.; Wettig, S. D.; Verrall, R. E. Interactions between 12-EO_x-12 Gemini Surfactants and Pluronic ABA Block Copolymers (F108 and P103) Studied by Isothermal Titration Calorimetry. *Langmuir* **2004**, *20*, 579–586.
(36) Li, X.; Wettig, S. D.; Verrall, R. E. Isothermal Titration Calorimetry and Dynamic Light Scattering Studies of Interactions between Gemini Surfactants of Different Structure and Pluronic Block Copolymers. *J. Colloid Interface Sci.* **2005**, *282*, 466–477.
(37) Bronich, T. K.; Popov, A. M.; Eisenberg, A.; Kabanov, V. A.; Kabanov, A. V. Effects of Block Length and Structure of Surfactant on Self-Assembly and Solution Behavior of Block Ionomer Complexes. *Langmuir* **2000**, *16*, 481–489.
(38) Kang, H.; Peng, B.; Liang, Y.; Han, X.; Liu, H. Study of the Interaction between a Diblock Polyelectrolyte PDMA-b-PAA and a Gemini Surfactant 12-6-12 in Basic Media. *J. Colloid Interface Sci.* **2009**, *333*, 135–140.

Received for review April 17, 2010. Accepted July 11, 2010. The authors acknowledge the financial support of the National High Technology Research and Development Program of China, Grant 2007AA090701-2; and the Important National Science and Technology Specific Project, Grant 2008ZX05024-002.

JE1003725